J. Fluid Mech. (1980), *vol.* 101, *part* 1, *pp.* 1–31
Printed in Great Britain

Onsager's pancake approximation for the fluid dynamics of a gas centrifuge

By HOUSTON G. WOOD

Union Carbide Corporation, Nuclear Division,
Oak Ridge, Tennessee

AND J. B. MORTON

University of Virginia, Charlottesville, Virginia

(Received 26 March 1979 and in revised form 6 February 1980)

A previously unpublished theory for describing the internal flow in a gas centrifuge is presented. The theory is based on boundary-layer-type arguments on the side walls of the centrifuge with the additional approximation of neglecting radial diffusion of radial momentum. The effects of the top and bottom end caps are incorporated through Ekman-layer solutions. The results are presented in a form amenable to numerical calculations.

Some sample calculations are presented for the special case of a centrifuge with a linear temperature profile on the wall and the top and bottom of the centrifuge at the same temperature as the corresponding end of the side wall.

1. Introduction

During the past few years, a large number of papers have appeared concerning flow in a gas centrifuge. This is no doubt related to the increased interest in gas centrifuges as a means of separating uranium isotopes. This work has mainly centred around the development of matched asymptotic expansions to represent the flow. Most of this work has been on the development of linearized models in which the flow is a small perturbation of a uniformly rotating isothermal gas.

While no attempt will be made here to give a complete survey of the literature, it is appropriate to summarize briefly some of the more important recent papers. Bark & Bark (1976) presented a uniformly valid asymptotic theory based on vertical boundary layers of thickness $E^{\frac{1}{4}}$ and $E^{\frac{1}{3}}$. These layers are of the Stewartson (1957) type. Brouwers (1978), using the same kind of analysis, considered flows induced by temperature differences, differential rotation, injection and removal of fluids at the ends and induced by temperature gradients on the cylinder walls. Matsuda & Hashimoto (1976) also considered Stewartson-layer flows. Their work included investigating the effects of insulated end plates, and insulated side walls. Also, three very good survey articles on gas centrifuges have been contributed by Olander (1972), Avery & Davies (1973) and Villani (1976). Another very good article that provides a good background on the separative processes of the gas centrifuge has been provided by Hoglund, Shacter & Von Halle (1979).

The purpose of this paper is to present a theory of the hydrodynamics of the flow in a gas centrifuge. This theory is the outgrowth of work that began in 1961 by a

0022–1120/80/4564–2260 $02.00

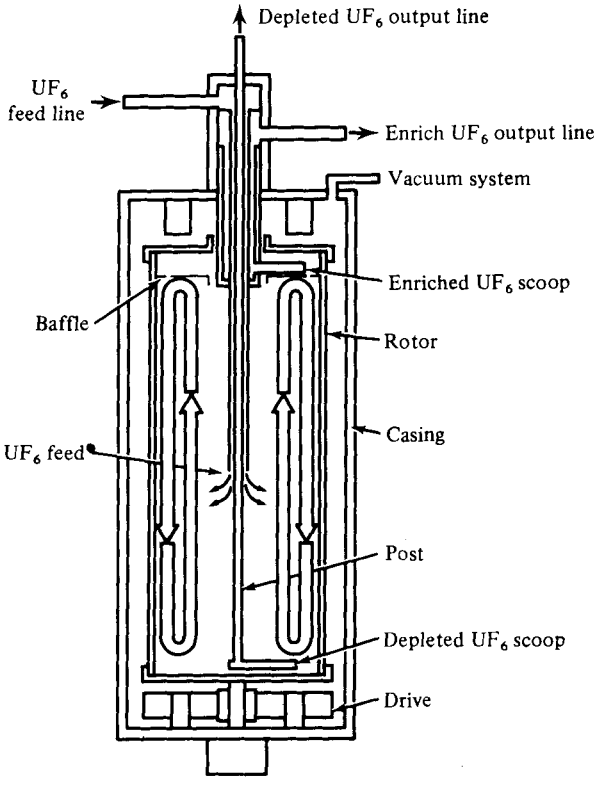

FIGURE 1. Gas centrifuge.

group of scientists led by the late Dr Lars Onsager. This group was formed under the auspices of the United States Atomic Energy Commission to develop a fundamental understanding of the flow processes in a gas centrifuge. Other members of the original group were George Carrier, Harvard University; Sterling Colgate, currently at the Los Alamos Scientific Laboratories; Wendell DeMarcus, University of Kentucky; the late Carl Eckart, Scripps Oceanographic Institute; Harold Grad, New York University; and Stephen Maslen, Martin Marietta.

The work presented in this paper is based primarily on an unpublished report by Onsager (1965, Approximate solutions of the linearized flow equations) on the 'pancake' approximation and on a report by Carrier & Maslen (1962) and presented in a paper by Carrier (1964) on the Ekman layers. The details of this theory were worked out and made amenable to numerical calculations by the authors and the late Hermon Parker of the University of Virginia.

In centrifuges of practical interest, rotation rates are sufficiently high that essentially all the gas is confined to a narrow annulus near the cylindrical wall (cf. figure 1). Counter-current gas centrifuges in which an axial convective circulation of the process gas is induced within the rotor in order to produce large end-to-end separation effects are the type of most interest (Von Halle 1977). For the model presented here, it will be assumed that this counter-current flow represents a small perturbation to the isothermal solid-body rotation. There are many physical mechanisms which can

drive these perturbations. These include an axial temperature gradient on the cylindrical wall, different end-cap temperatures, end caps rotating at speeds slightly different from that of the centrifuge, mass injection from any of the boundaries, and stationary obstacles inserted into the flow.

In § 2 of this paper, the basic theory is presented along with the derivation of the equations. The equations are derived in a very general form and include the effects of sources of mass, momentum and energy. These source terms are not retained in the subsequent analysis but will be dealt with in a future paper. Section 3 presents a general discussion of the problem and its boundary conditions. It is shown that the complete solution can be represented by sums of three types of terms, i.e. the 'zero eigenfunction', the end-driven modes, and the lateral modes. The end-driven modes are discussed in § 4 while § 5 presents the lateral modes and the zero eigenfunction. The Ekman boundary layers at the ends of the bowl are discussed in § 6 and some numerical results are presented in § 7.

2. Derivation of the equations for the cylindrical boundary layer

2.1. *The reference solution*

Let (r, θ, z) be cylindrical polar co-ordinates with the origin fixed in the bottom of the centrifuge on the axis of rotation, and let (U, V, W) be the corresponding components of velocity. The z axis lies along the axis of the right circular cylinder which is rotating at an angular velocity Ω. If the fluid is rotating as a solid body, then the velocity components are given by

$$U = 0, \quad V = \Omega r, \quad W = 0, \tag{2.1}$$

and the pressure distribution is governed by the hydrostatic equation

$$\frac{d\hat{p}}{dr} = \hat{\rho} r \Omega^2, \tag{2.2}$$

where $\hat{p}$ is the pressure and $\hat{\rho}$ is the density.

For a perfect gas at uniform temperature, T_0, the pressure distribution in the cylinder is

$$\hat{p} = p_w \exp\{-A^2[1-(r/a)^2]\}, \tag{2.3}$$

where a is the radius of the cylinder, $A = a\Omega/(2RT_0)^{\frac{1}{2}}$, R is the gas constant, and p_w is the pressure on the cylinder wall.

2.2. *Linearized equations*

Let (u', v', w') be perturbations of the reference velocity components (U, V, W) with p', ρ', and T' the corresponding perturbations of the pressure $\hat{p}$, density $\hat{\rho}$, and temperature T_0. For steady axisymmetric motions the first-order perturbation equations for conservation of mass, momentum, energy and state are

$$\frac{1}{r}(r\hat{\rho}u')_r + \hat{\rho}w'_z = 0, \tag{2.4}$$

$$-2\Omega\hat{\rho}v' - r\Omega^2\rho' = -p'_r + \frac{4\mu}{3}\left[\frac{1}{r}(ru'_r)_r - \frac{u'}{r^2}\right] + \mu u'_{zz} + \frac{\mu}{3}w'_{zr}, \tag{2.5}$$

$$2\Omega\hat{\rho}u' = \mu\left[\frac{1}{r}(rv'_r)_r + v'_{zz} - \frac{v'}{r^2}\right], \tag{2.6}$$

$$0 = -p'_z + \frac{\mu}{r}(rw'_r)_r + \frac{4\mu}{3}w'_{zz} + \frac{\mu}{3r}(ru')_{rz}, \tag{2.7}$$

$$0 = r\Omega^2\hat{\rho}u' + k\left[\frac{1}{r}(rT'_r)_r + T'_{zz}\right], \tag{2.8}$$

$$p' = \hat{\rho}RT' + \rho' RT_0, \tag{2.9}$$

where k is the thermal conductivity and μ is the viscosity and where the bulk viscosity has been taken to be 0. Let $\bar{\Delta}$ be the Laplace operator and use equations (2.2) and (2.4) to rewrite equations (2.5) and (2.7) as

$$-2\Omega\hat{\rho}v' - r\Omega^2\rho' = -p'_r + \mu\left[\bar{\Delta}u' - \frac{u'}{r^2} - \frac{\Omega^2}{3RT_0}(ru')_r\right], \tag{2.5a}$$

$$p'_z = \mu\left[\bar{\Delta}w' - \frac{\Omega^2 r}{3RT_0}u'_z\right]. \tag{2.7a}$$

It is convenient to consider the equations in dimensionless form and we do so by calling $\eta = r/a, y = z/a, Re = \rho_w\Omega a^2/\mu, u = u'/\Omega a, w = w'/\Omega a, \omega = v'/\Omega r, \rho_0 = \hat{\rho}/\rho_w$, $\rho = \rho'/\rho_w, p = p'/p_w, \theta = T'/T_0$, where ρ_w and p_w are the density and pressure at the vertical wall of the cylinder. Let Δ be the Laplace operator in dimensionless coordinates and the equations (2.4) to (2.9) become

$$(\eta\rho_0 u)_\eta + \eta\rho_0 w_y = 0, \tag{2.10}$$

$$-2\eta\rho_0\omega - \eta\rho = -\frac{1}{2A^2}p_\eta + \frac{1}{Re}\left[\Delta u - \frac{u}{\eta^2} - \frac{2A^2}{3}(\eta u)_\eta\right], \tag{2.11}$$

$$2\rho_0 u = \frac{1}{Re}\left[\Delta(\eta\omega) - \frac{\omega}{\eta}\right], \tag{2.12}$$

$$p_y = \frac{2A^2}{Re}\left[\Delta w - \frac{2A^2}{3}\eta u_y\right], \tag{2.13}$$

$$0 = 4\,Re\,(S-1)\,(\eta\rho_0 u) + \Delta\theta, \tag{2.14}$$

$$p = \rho + \rho_0\theta, \tag{2.15}$$

where $S = 1 + Pr\,A^2(\gamma-1)/2\gamma$, $Pr = C_p\mu/k$ is the Prandtl number and C_p is the specific heat at constant pressure.

2.3. *Onsager's differential equation*

A boundary-layer analysis based on the assumption that $Re \gg 1$ implies that the fluid dynamics in the cylinder may be characterized by examining three principal regions: an internal flow region where the axial diffusion terms are negligible and Ekman layers at the top and bottom of the cylinder where axial diffusion is important. The goal of this section is to explain the approximations used to reduce the system of equations (2.10) to (2.15) to a single partial differential equation valid in the region away from the ends of the cylinder.

For $A^2 \gg 1$, the radial extent of the bowl over which the dynamics is of interest is very near the wall. If we set $\eta = 1$ where it appears algebraically, equations (2.12) and (2.14) combine to give

$$\Delta[\theta + 2(S-1)\omega] = 0 \tag{2.16}$$

and

$$\Delta(\theta - 2\omega) = -4\,Re\,S\rho_0 u. \tag{2.17}$$

Using equation (2.15) to eliminate ρ from equation (2.11) yields

$$\eta\rho_0(\theta - 2\omega) = \eta p - \frac{1}{2A^2}p_\eta + \frac{1}{Re}\left[\Delta u - \frac{u}{\eta^2} - \frac{2A^2}{3}(\eta u)_\eta\right]. \tag{2.18}$$

In view of the last two equations, we define the quantity $\phi = \theta - 2\omega$. The system is described by equations (2.10), (2.13), (2.16), (2.17) and (2.18). In the region of the cylinder away from the ends we retain among the viscous terms only those most highly differentiated in the radial direction and introduce the new radial variable $x = A^2(1-\eta^2)$ which measures distance from the rotor wall in scale heights (*e*-folding heights) of the ambient density. By including sources terms, we can study the effects of sources and sinks of mass, momentum and energy interior to the fluid as well as on the boundaries. When this is done, the appropriate approximate model is described by the following system of equations:

$$e^{-x}w_y - 2A^2(e^{-x}u)_x = \mathscr{M}, \tag{2.19}$$

$$\phi = (e^x p)_x + e^x \mathscr{U}, \tag{2.20}$$

$$\phi_{xx} = -\frac{Re\,S}{A^4}e^{-x}u - (\mathscr{T} - 2\mathscr{V}), \tag{2.21}$$

$$p_y = \frac{8A^6}{Re}w_{xx} + \mathscr{W}, \tag{2.22}$$

$$-4A^4 h_{xx} - h_{yy} = \mathscr{T} + 2(S-1)\mathscr{V}, \tag{2.23}$$

where $\mathscr{M}, \mathscr{U}, \mathscr{V}, \mathscr{W}, \mathscr{T}$ are sources or sinks of mass, three components of momentum, and energy, respectively. The non-dimensionalizing factors for these terms are $\rho_w\Omega$, $\rho_w\Omega^2 a$, $4A^4\Omega\mu/a$, $\rho_w RT_0/a$, and $4A^4 kT_0/a^2$, respectively. We also define

$$h = \theta + 2(S-1)\omega.$$

Eliminating p between equations (2.20) and (2.22), we get

$$\phi_y = \frac{8A^6}{Re}(e^x w_{xx})_x + (e^x\mathscr{W})_x + e^x\mathscr{U}_y. \tag{2.24}$$

In order to allow for mass sources and sinks, we define a stream function in two parts, ψ and $\bar{\psi}$, by the relations

$$e^{-x}u = -\psi_y - \frac{1}{2A^2}\bar{\psi} \tag{2.25}$$

and

$$e^{-x}w = -2A^2\psi_x. \tag{2.26}$$

By substituting these two quantities in equation (2.19), we find $\overline{\psi}_x = \mathscr{M}$ and, imposing the boundary conditions $u(0,y) = 0$ and $\psi(0,y) = 0$, we find that $\overline{\psi}(0,y) = 0$; hence

$$\overline{\psi}(x,y) = \int_0^x \mathscr{M}(x',y)\,dx'. \tag{2.27}$$

Thus in the case $\mathscr{M} \equiv 0$ (no mass source), ψ becomes the usual stream function. Introducing the stream function in equations (2.21) and (2.24) yields

$$\phi_{xx} = \frac{Re\,S}{A^4}\psi_y + \frac{Re\,S}{2A^6}\int_0^x \mathscr{M}(x',y)\,dx' - (\mathscr{T} - 2\mathscr{V}) \tag{2.28}$$

and

$$\phi_y = \frac{-16A^8}{Re}(e^x(e^x\psi_x)_{xx})_x + (e^x\mathscr{W})_x + e^x\mathscr{U}_y. \tag{2.29}$$

Now equations (2.23), (2.28) and (2.29) govern the system. Either ϕ or ψ may be eliminated between the last two of these equations and we choose to eliminate ϕ in favour of ψ. This yields

$$(e^x(e^x\psi_x)_{xx})_{xxx} + \frac{Re^2S}{16A^{12}}\psi_{yy} = F_x(x,y), \tag{2.30}$$

where

$$F_x(x,y) = \frac{Re}{16A^8}(e^x\mathscr{W})_{xxx} + \frac{Re}{16A^8}(e^x\mathscr{U}_y)_{xx} - \frac{Re^2S}{32A^{14}}\overline{\psi}_y + \frac{Re}{16A^8}(\mathscr{T} - 2\mathscr{V})_y. \tag{2.31}$$

We follow Onsager and introduce a potential function by the relation $\psi = -2A^2\chi_x$. After integrating once with respect to x, equation (2.30) becomes

$$(e^x(e^x\chi_{xx})_{xx})_{xx} + B^2\chi_{yy} = F(x,y), \tag{2.32}$$

where

$$F(x,y) = \frac{B^2A^2}{2\,Re\,S}\int_x^\infty (\mathscr{T}_y - 2\mathscr{V}_y)\,dx' - \frac{B^2}{4A^4}\int_x^\infty\int_0^{x'} \mathscr{M}_y\,dx''\,dx'$$

$$- \frac{B^2A^2}{2\,Re\,S}[(e^x\mathscr{U}_y)_x + (e^x\mathscr{W})_{xx}] \tag{2.33}$$

and

$$B = \frac{Re\,S^{\frac{1}{2}}}{4A^6}.$$

The solution of equation (2.32) yields ψ and ϕ, which is sufficient in many cases. However, if one wishes to decouple θ and ω, equation (2.23) must also be solved for h.

A number of differential operators are frequently used and we will simplify the notation by making the following definitions

$$Lf(x) = [e^x(e^xf_{xx})_{xx}]_{xx}, \quad L_1f(x) = f_x, \quad L_2f(x) = e^xf_{xx},$$

$$L_3f(x) = [e^xf_{xx}]_x, \quad L_4f(x) = [e^xf_{xx}]_{xx}, \quad L_5f(x) = [e^x(e^xf_{xx})_{xx}]_x.$$

Several physical variables are expressed in terms of the master potential χ in the appendix.

3. General discussion of solution

3.1. *Decomposition of solution*

For the remainder of this paper we will assume there are no internal sources and study the homogeneous form of Onsager's equation

$$[e^x(e^x\chi_{xx})_{xx}]_{xx} + B^2\chi_{yy} = 0 \tag{3.1}$$

and a particular motion to which it is applicable.

We seek solutions to equation (3.1) of the form

$$\chi(x, y) = f(x)\, g(y). \tag{3.2}$$

Inserting (3.2) into (3.1) leads to two equations: one for f and one for g. These equations are

$$[e^x(e^x f_{xx})_{xx}]_{xx} + \lambda^2 f = 0 \tag{3.3}$$

and

$$B^2 g_{yy} - \lambda^2 g = 0, \tag{3.4}$$

where λ^2 is the separation constant. There are three distinct and useful classes of solutions to these equations corresponding to λ real, λ purely imaginary, and $\lambda = 0$.

Case 1: λ *purely imaginary.* Letting $\beta = i\lambda/B$, then β is real and equation (3.4) becomes

$$g_{yy} + \beta^2 g = 0. \tag{3.5}$$

The solution of (3.5) is

$$g(y) = A\cos\beta y + C\sin\beta y.$$

As will be shown in § 5 these solutions, called lateral modes, form a complete set of functions which can be used to satisfy temperature boundary conditions on the wall of the centrifuge.

Case 2: $\lambda = 0$. The solution of equation (3.4) with $\lambda = 0$ is

$$g(y) = A + Cy. \tag{3.6}$$

These solutions, called the zero eigenfunctions, are also useful in satisfying some simple boundary conditions on the walls. For example, it will be seen in § 5.1 that, if the temperature varies linearly on the wall, the $\lambda = 0$ solutions and not the purely imaginary λ solutions are used.

Case 3. λ *real.* Letting $\alpha = \lambda/B$, then equation (3.4) becomes

$$g_{yy} - \alpha^2 g = 0. \tag{3.7}$$

The solution of this equation is

$$g = A\, e^{-\alpha y} + C\, e^{+\alpha y}.$$

It will be shown in § 4 that these solutions, called end modes, are useful in satisfying the boundary conditions at the top and bottom of the bowl.

It will be shown in § 6 that the effect of Ekman layers on the internal flow region can be replaced by a boundary condition and that the λ-real solutions are useful in satisfying these boundary conditions.

Since the basic equation (3.1) is linear, we can use superposition of the three basic types of solutions to satisfy any general boundary condition.

3.2. *Boundary conditions*

At the rotor wall, the boundary conditions on equation (3.1) require that the radial and axial velocities be zero; and ϕ_y, which represents a combination of azimuthal velocity and temperature gradients along the wall, is an arbitrary specified function. Of course, since the no-slip conditions apply, ϕ_y becomes the temperature gradient on the wall.

In terms of the potential function, these boundary conditions are

$$\chi_x(0,y) = \chi_{xx}(0,y) = 0,$$

$$L_5\chi(0,y) = \frac{Re}{32A^{10}}\bar{\phi}_y(y), \tag{3.8}$$

where $\bar{\phi}(y)$ is a prescribed function. As $x \to \infty$, we impose the boundary conditions $u = w_x = \phi_x = 0$, which can be expressed in terms of the potential function as

$$\chi_y(\infty,y) = \chi_x(\infty,y) = L_3\chi(\infty,y) = 0. \tag{3.9}$$

For centrifuges with feed along the axis, these conditions are altered. The boundary conditions at the top and bottom of the centrifuge require that the internal flow solution matches the Ekman-layer solution. This will be discussed in detail in § 6.

4. End-driven modes

4.1. *Introduction*

In this section, the end-driven modes will be discussed in detail. In subsection 4.2, equation (3.3) and the appropriate boundary conditions will be shown to be self-adjoint. The orthogonality conditions for the eigenfunctions are also derived.

The eigenvalues and eigenfunctions are then computed in the next two subsections. In subsection 4.3 a direct numerical procedure is presented and in subsection 4.4 an asymptotic procedure is discussed.

4.2. *Self-adjoint*

The basic equation for x dependence of the end-driven modes is

$$[e^x(e^x f_{xx})_{xx}]_{xx} + B^2\alpha^2 f = 0. \tag{4.1}$$

It is useful to show that this equation together with its boundary conditions is self-adjoint and to derive the orthogonality relations between the eigenfunctions. The appropriate boundary conditions are

$$f_x(0) = f_{xx}(0) = L_5 f(0) = 0,$$

$$f(\infty) = f_x(\infty) = L_3 f(\infty) = 0. \tag{4.2}$$

Let f_1 and f_2 be two solutions of (4.1) subject to the appropriate boundary conditions corresponding to different eigenvalues $B\alpha_1$ and $B\alpha_2$ respectively. By assumption,

$$[e^x(e^x f_{1xx})_{xx}]_{xx} + B^2\alpha_1^2 f_1 = 0.$$

Multiplying by f_2 and integrating from 0 to ∞ yields

$$\int_0^\infty f_2[e^x(e^x f_{1xx})_{xx}]_{xx}\,dx + B^2\alpha_1^2\int_0^\infty f_1 f_2\,dx = 0.$$

Integrating the first term by parts three times and using the boundary conditions yields

$$-\int_0^\infty (e^x f_{2xx})_x\,(e^x f_{1xx})_x\,dx + B^2\alpha_1^2\int_0^\infty f_1 f_2\,dx = 0.$$

Repeating this on an equation for f_2 multiplied by f_1 yields

$$-\int_0^\infty (e^x f_{1xx})_x\,(e^x f_{2xx})_x\,dx + B^2\alpha_1^2\int_0^\infty f_1 f_2\,dx = 0.$$

Subtracting these two equations, we get

$$B^2(\alpha_1^2-\alpha_2^2)\int_0^\infty f_1 f_2\,dx = 0. \tag{4.3}$$

These results show that the differential equation (4.1) with the boundary conditions (4.2) is self-adjoint and the eigenfunctions are orthogonal as shown by equation (4.3).

Since the differential equation (4.1) is self-adjoint we can express the eigenvalues in terms of a minimum principle (Courant & Hilbert 1953).

Let

$$I = \int_0^\infty \frac{e^{2x}}{2}\{f_{xxx}+f_{xx}\}^2\,dx$$

and

$$J = \frac{1}{2}\int_0^\infty f^2\,dx.$$

Then

$$\alpha B = \min\frac{I}{J},$$

where the minimum is over all functions satisfying the boundary conditions (4.2).

4.3. *Direct numerical calculation*

Let $t = x-\log(\alpha B)$ and substitute into equation (4.1). The process yields

$$[e^t(e^t f_{tt})_{tt}]_{tt}+f = 0. \tag{4.4}$$

Using the method of Frobenius, Onsager solved this equation and showed that only three of its six solutions satisfy the boundary conditions at $x\to\infty$. These are

$$f_1(t) = \sum_{n=1}^{\infty}\frac{(-1)^n e^{-2nt}}{2^{2n}[(2n)!\,(n-1)!]^2},$$

$$f_2(t) = \sum_{n=1}^{\infty}\frac{(-t-\sigma(n))\,(-1)^n e^{-2nt}}{2^{2n}[(2n)!\,(n-1)!]^2},$$

$$f_3(t) = \sum_{n=0}^{\infty}\frac{(-1)^n e^{-(2n+1)t}}{2^{(2n+1)}[(2n+1)!\,(n-\frac{1}{2})!]^2},$$

Number	$t = -\log(\alpha B)$
1	−0·8800138
2	−2·714864
3	−3·792559
4	−4·576250
5	−5·194949
6	−5·706744
7	−6·143383
8	−6·524416
9	−6·860389
10	−7·182411

TABLE 1. First 10 eigenvalues for the end-driven modes.

where

$$\sigma(n) = \sigma(n-1) + \frac{6n(n-1)+1}{n(n-1)(2n-1)}$$

and

$$\sigma(1) = 1{\cdot}96150018\ldots$$

($\sigma(1) = 3 - 3\gamma + \log 2$, where γ is Euler's number). Thus a general solution of equation (4.4) which satisfies the boundary conditions at $x = \infty$ can be written as

$$f(t) = A_1 f_1(t) + A_2 f_2(t) + A_3 f_3(t).$$

At $x = 0$, $t = -\log(\alpha B)$ the boundary conditions are expressed

$$\begin{pmatrix} f_{1t} & f_{2t} & f_{3t} \\ f_{1tt} & f_{2tt} & f_{3tt} \\ L_5 f_1 & L_5 f_2 & L_5 f_3 \end{pmatrix} \begin{pmatrix} A_1 \\ A_2 \\ A_3 \end{pmatrix} = 0 \quad \text{at} \quad t = -\log(\alpha B). \tag{4.5}$$

This set of homogeneous equations has solutions only if the determinant of the coefficient matrix is zero. This occurs only at discrete values of $\log(\alpha B)$. When this happens, equation (4.5) determines only the ratio of A_1, A_2 and A_3. Thus

$$f = A_1 f_1 + A_2 f_2 + A_3 f_3 \tag{4.6}$$

is arbitrary to a multiplicative constant. The values of t for which this happens will be referred to as eigenvalues and the corresponding f's as eigenfunctions. The results of these calculations are presented in table 1 and figures 2–5. In table 1 are listed the first ten values of $\log(\alpha B)$. Figure 2 shows the first four eigenfunctions, figures 3, 4 and 5 show the first, second and L_5 derivatives of these eigenfunctions.

Letting t_n and f_n be corresponding eigenvalue–eigenfunction pairs (modes) arranged so that t_n are in increasing order and recalling that $\alpha = e^{-t_n}/B$, we can write the general solution for the end-driven modes as

$$\chi_E = \sum_{n=1}^{\infty} (D_n f_n(x)\, e^{-\alpha_n y} + E_n f_n(x) e^{\alpha_n (y - y_0)}), \tag{4.7}$$

where y_0 is the normalized length of the rotor.

Physically, $1/\alpha_n$ represents the decay length for the nth mode. That is, if $D_n = 1$ and all other D's and E's are zero, then the nth mode will be reduced in amplitude by a factor of $1/e$ in a distance $1/\alpha_n$.

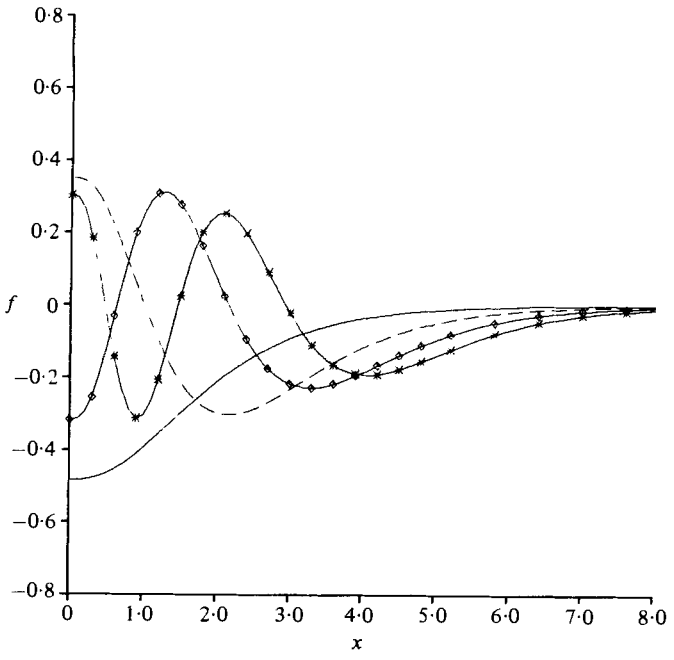

FIGURE 2. First four end-driven eigenfunctions: ——, mode 1; – – –, mode 2; ◇, mode 3; *, mode 4.

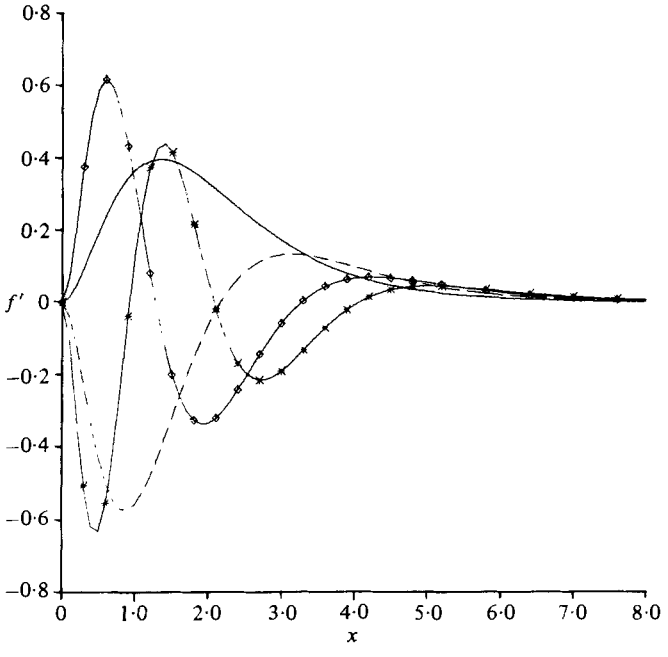

FIGURE 3. First derivative of the first four end-driven eigenfunctions: ——, mode 1; – – –, mode 2; ◇, mode 3; *, mode 4.

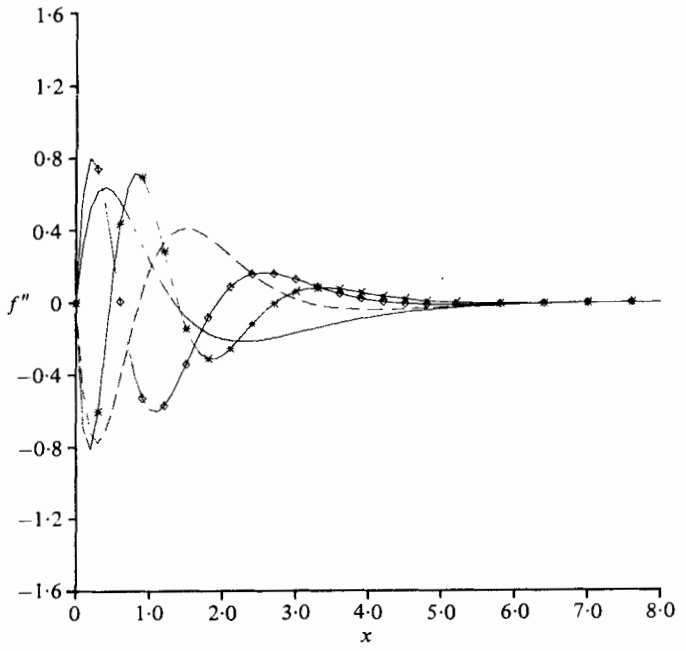

FIGURE 4. Second derivative of the first four end-driven eigenfunctions: ——, mode 1; – – –, mode 2; ◇, mode 3; *, mode 4.

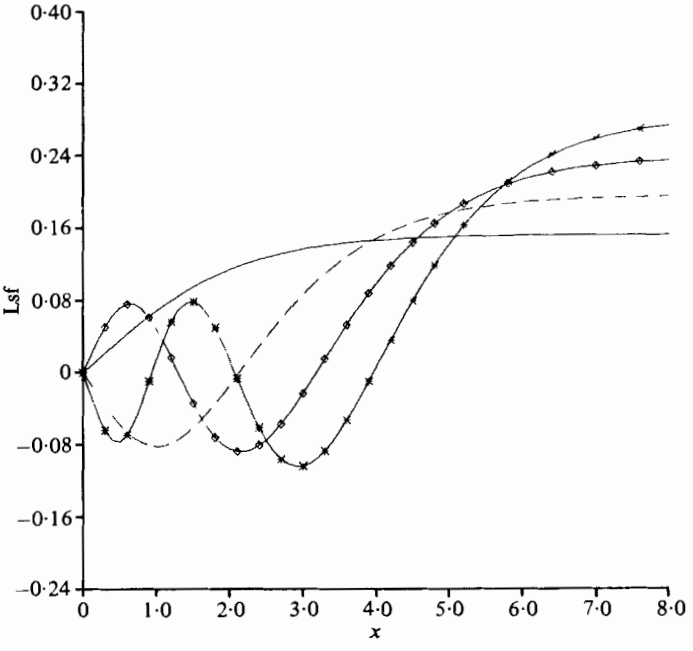

FIGURE 5. L_5 derivative of the first four end-driven eigenfunctions: ——, mode 1; – – –, mode 2; ◇, mode 3; *, mode 4.

n	α_1/α_n
1	1
2	0·159637
3	0·054337
4	0·024817
5	0·013367
6	0·008013
7	0·005178
8	0·00354
9	0·00253
10	0·00183

TABLE 2. Ratio of decay lengths for the first 10 eigenfunctions.

It is useful to look at the ratios α_1/α_n. These ratios give the relative decay lengths of the nth mode to the first mode. As can be seen from table 2, the decay lengths drop off quite rapidly compared to the first mode.

4.4. *Asymptotic eigenfunctions and eigenvalues*

The end-driven eigenfunctions become increasingly difficult to calculate for larger eigenvalues using the methods discussed in the previous section. This is due to the fact that basic solutions used become increasingly similar so that the eigenfunctions must be calculated as small differences between increasingly large numbers. If more eigenfunctions are needed, asymptotic methods must be used. The purpose of this section is to describe the appropriate asymptotic calculation.

The fundamental equation to be solved is

$$\{e^x[e^x f_{xx}]_{xx}\}_{xx} + B^2\alpha^2 f = 0. \tag{4.8}$$

Letting

$$\epsilon^6 = 1/(\alpha^2 B^2), \tag{4.9}$$

we will look for a solution of the form

$$f(x) = e^{q(x,\epsilon)/\epsilon}, \tag{4.10}$$

where

$$q(x,\epsilon) = q_0(x) + \epsilon q_1(x) + \epsilon^2 q_2(x) + \dots . \tag{4.11}$$

Substituting (4.10) into (4.8) and performing the indicated operations and equating orders of ϵ leads to the following equations:

Order ϵ^0

$$q_0'^6 + e^{-2x} = 0; \tag{4.12}$$

Order ϵ^1

$$15q_0'^4 q_0'' + 6q_1' q_0'^5 + 6q_0'^5 = 0. \tag{4.13}$$

From equation (4.12)

$$q_0' = (-1)^{\frac{1}{6}} e^{-\frac{1}{3}x}, \tag{4.14}$$

where the six roots of (-1) are

$$\tfrac{1}{2}(\sqrt{3}+i), \quad i, \quad \tfrac{1}{2}(-\sqrt{3}+i), \quad \tfrac{1}{2}(-\sqrt{3}-i), \quad -i, \quad \tfrac{1}{2}(\sqrt{3}-i).$$

Solving equation (4.13) for q_1' gives

$$q_1' = -\left(1+\frac{15}{6}\frac{q_0''}{q_0'}\right).$$

Using (4.14) to evaluate q_0', q_0'' yields

$$q_1' = -\tfrac{1}{6}$$

or

$$q_1 = -\frac{x}{6}.$$

Thus, to order ϵ^2, the asymptotic eigenfunction becomes

$$\begin{aligned} f_{\text{asy}} \sim e^{-\frac{1}{6}x}\{&A_0\cos(3\epsilon^{-1}e^{-\frac{1}{3}x}+\delta)\\ &+B_0\exp(-\tfrac{1}{2}3^{\frac{3}{2}}\epsilon^{-1}e^{-\frac{1}{3}x})\cos(\tfrac{3}{2}\epsilon^{-1}e^{-\frac{1}{3}x}+\beta)\\ &+C_0\exp(\tfrac{1}{2}3^{\frac{3}{2}}\epsilon^{-1}e^{-\frac{1}{3}x})\cos(\tfrac{3}{2}\epsilon^{-1}e^{-\frac{1}{3}x}+\gamma)\}. \end{aligned} \tag{4.15}$$

Letting $\epsilon^{-1} = e^{\frac{1}{3}a}$ and $\nu = \frac{1}{2}3^{\frac{3}{2}} = 2{\cdot}598076\ldots$,

$$\begin{aligned} f_{\text{asy}} \sim e^{-\frac{1}{6}x}\{&A_0\cos(3e^{\frac{1}{3}(a-x)}+\delta)\\ &+B_0\exp[-\nu e^{\frac{1}{3}(a-x)}]\cos(\tfrac{3}{2}e^{\frac{1}{3}(a-x)}+\beta)\\ &+C_0\exp[\nu e^{\frac{1}{3}(a-x)}]\cos(\tfrac{3}{2}e^{\frac{1}{3}(a-x)}+\gamma)\}. \end{aligned} \tag{4.16}$$

The appropriate boundary conditions that this solution must satisfy are

$$\begin{aligned} f'(0) = 0, \quad & f(\infty) = 0,\\ f''(0) = 0, \quad & f'(\infty) = 0,\\ L_5 f(0) = 0, \quad & L_3 f(\infty) = 0. \end{aligned} \tag{4.17}$$

Because of the exponential dependence of the second term, we will assume that it is negligible except near infinity. The boundary conditions at $x = 0$ are used to determine the remaining parameters. Note that, since the boundary conditions are homogeneous, one of the parameters is arbitrary. Thus we choose $A_0 = 1$.

Let

$$y = \epsilon^{-1}(e^{-\frac{1}{3}x}-1).$$

Then

$$f_{\text{asy}} = e^{-\frac{1}{6}x}\{\cos[3y+\delta+3\epsilon^{-1}]+C_0\,e^{\nu\epsilon^{-1}}e^{\nu y}\cos[\tfrac{3}{2}y+(\gamma+\tfrac{3}{2}\epsilon^{-1})]\}. \tag{4.18}$$

Substituting equation (4.18) into the boundary conditions at $x = 0$ yields after much algebra

$$\begin{aligned} \delta &= -\tfrac{1}{4}\pi,\\ \gamma &= \frac{n\pi}{2}+\frac{7\pi}{24}+O\left(\frac{1}{n^2}\right),\\ \epsilon^{-1} &= \frac{\pi}{3}\left(n+\tfrac{5}{12}+\frac{1}{2\pi^2 n}+\ldots\right),\\ C_0 &= \left(-1+\frac{\sqrt{3}}{4\pi n}\right)e^{-\gamma/\epsilon}. \end{aligned}$$

n	Direct calculation	Asymptotic calculation
5	5·19495	5·21240
6	5·70674	5·71899
7	6·14338	6·15246
8	6·524416	6·53125
9	6·860388	6·867589

TABLE 3. Comparison of eigenvalues.

n	x_d	x_c
0	∞	7·60
1	5·22	5·05
2	3·75	3·69
3	2·79	2·75
4	2·07	2·05
5	1·49	1·48
6	1·00	1·02
7	0·590	0·580
8	0·210	0·230

TABLE 4. Comparison of zeros for the ninth eigenfunction calculated directly and from the asymptotic eigenfunction.

Table 3 compares the results of the asymptotic analysis with the values for the eigenvalue calculated in the previous section. The values in the table represent the $\log(\alpha B)$, where αB is defined in equation (4.8). It should be pointed out that this eigenfunction does not satisfy the boundary conditions at ∞. Near $x = \infty$, the term which was neglected (second term of equation (4.16)) must be included. However, since in gas centrifuges of practical importance most of the gas is confined to a very narrow region near the wall, this term is of no real significance.

To compare the asymptotic eigenfunctions with the direct calculation, it is useful first to compare the zeros of the two calculations. Table 4 compares the zeros for the ninth eigenfunction calculated directly (x_d) with the zeros from the asymptotic eigenfunctions (x_c) given by equation (4.18).

5. Lateral modes

5.1. *Zero eigenfunction*

We consider equation (3.1) for the case $\lambda = 0$ and call the solution the zero eigenfunction. Parker (1973, The with-feed pancake model of internal flow in a gas centrifuge, unpublished manuscript) was the first to make use of this solution, which we write with this notation

$$\chi_0(x, y) = (b_0 + c_0 y) + (b_3 + c_3 y)\, h_3(x) + (b_5 + c_5 y)\, h_5(x) + (P_0 + P_z y)\, h_p(x), \qquad (5.1)$$

where

$$h_3(x) = x\,e^{-x} + \tfrac{1}{2}e^{-2x},$$

$$h_5(x) = -2\,e^{-x} + \tfrac{3}{2}e^{-2x} + x\,e^{-2x},$$

$$h_p(x) = \tfrac{1}{2}x + e^{-x} - \tfrac{1}{4}e^{-2x}.$$

Since all physical quantities are related to derivatives of the master potential, we choose to set $b_0 = 0$. For the case of a centrifuge with no feed being introduced at the axis, $\chi_0(x, y)$ satisfies the boundary condition at $x = \infty$ given by equation (3.9) when $c_0 = b_3 = c_3 = P_0 = P_z = 0$. The solution $\chi_0(x, y)$ also satisfies the velocity boundary conditions at $x = 0$ given by equation (3.8) and the temperature boundary conditions gives

$$L_5\chi_0(0, y) = 4(b_5 + c_5 y) = \frac{Re}{32A^{10}}\theta_y(0). \tag{5.2}$$

Therefore, if the temperature of the rotor wall is a quadratic or linear function of y, $\chi_0(x, y)$ satisfies the boundary conditions exactly. Since $\rho_0 w = 4A^4\chi_{xx}$ we find from the zero eigenfunction that

$$w = -8A^4 b_5[1 - (1 + 2x)\,e^{-x}],$$

which corresponds to the idealized flow model obtained by Parker & Kelly (1967, The universal high-speed flow pattern: centrifuge performance based on the rod-like solution, unpublished manuscript) and independently and more recently by Lotz (1973).

5.2. *Series solutions*

For the case of λ purely imaginary as discussed in case 1 of § 3 we see that the basic equation for laterally driven modes is

$$[e^x(e^x f_{xx})_{xx}]_{xx} - \beta^2 B^2 f = 0. \tag{5.3}$$

Let $s = x - \log(\beta B)$ and substitute in equation (5.3) to get

$$[e^s(e^s f_{ss})_{ss}]_{ss} - f = 0. \tag{5.4}$$

As in § 4, the method of Frobenius yields six solutions to the differential equation. For completeness we will list these solutions here. The coefficients involve the digamma and polygamma functions which we will tabulate first:

$$\Gamma(\tfrac{1}{2}) = \sqrt{\pi},$$

$$-\psi(0) = \gamma \quad \text{(Euler's constant)},$$

$$-\psi(-\tfrac{1}{2}) = \gamma + \log 4,$$

$$\psi(n) - \psi(n-1) = 1/n,$$

$$\psi'(0) = \pi^2/6,$$

$$\psi'(n-1) - \psi'(n) = 1/n^2, \quad \psi'(\infty) = 0,$$

$$-\psi''(0) = 2\zeta(3) = 2{\cdot}404113806,$$

$$\psi''(n) - \psi''(n-1) = 2/n^3, \quad \psi''(\infty) = 0.$$

For simplification,

$$\sigma(n) = 2\psi(2n) + \psi(n-1) + \log 2,$$

$$\sigma_1(n) = 2\psi'(2n) + \tfrac{1}{2}\psi'(n-1),$$

$$\sigma_2(n) = 2\psi''(2n) + \tfrac{1}{4}\psi''(n-1).$$

These recurrence formulae are as used by Onsager, but one might note that most references such as Erdélyi (1953) use the initial value $\psi(1) = -\gamma$. We will also define

$$b_k = [2^k \Gamma(2k+1)\,\Gamma(k)]^{-2},$$

$$d_k = [2^{k+\frac{1}{2}} \Gamma(2k+2)\,\Gamma(k+\tfrac{1}{2})]^{-2}.$$

Onsager's solutions can now be written as

$$\mathscr{S}_1(s) = \sum_{k=1}^{\infty} b_k e^{-2ks},$$

$$\mathscr{S}_2(s) = \sum_{k=1}^{\infty} b_k(-s-\sigma(k))\, e^{-2ks},$$

$$\mathscr{S}_3(s) = \tfrac{1}{2} + \sum_{k=1}^{\infty} b_k[(s+\sigma(k))^2 - \sigma_1(k)]\, e^{-2ks},$$

$$\mathscr{S}_4(s) = \tfrac{3}{2}(-s+3\gamma-\log 2) - \sum_{k=1}^{\infty} b_k[(s+\sigma(k))^3 - 3\sigma_1(k)\,(s+\sigma(k)) + \sigma_2(k)]\, e^{-2ks},$$

$$\mathscr{S}_5(s) = \sum_{k=0}^{\infty} d_k e^{-(2k+1)s},$$

$$\mathscr{S}_6(s) = \sum_{k=0}^{\infty} d_k[-s-\sigma(k+\tfrac{1}{2})]\, e^{-(2k+1)s}.$$

In terms of the variable x, we use the notation

$$S_{jn}(x) \equiv \mathscr{S}_j(s) = \mathscr{S}_j[x - \log(B\beta_n)],$$

where $j = 1, 2, \ldots, 6$ and $n = 1, 2, 3, \ldots$; therefore the functions $S_{jn}(x)$ satisfy the differential equation

$$LS_{jn}(x) = \beta_n^2 B^2 S_{jn}(x).$$

5.3. *Boundary conditions*

These modes can be used to satisfy arbitrary boundary conditions at the rotor wall, and/or at some interior radius, X_T, in the case of feed from the axis or in the case of a concentric inner cylinder. The axial dependence can be expressed by trigonometric functions as discussed in § 3 and, for convenience, we make the approximation $\beta = 2n\pi/y_0$, which will be compensated for by the Ekman-layer matching discussed in § 6. Therefore, the general solution for the laterally driven modes is given by

$$x_L = \sum_{n=1}^{\infty} \sum_{j=1}^{6} S_{jn}(x) \left[a_{jn} \cos\left(\frac{2n\pi y}{y_0}\right) + b_{jn} \sin\left(\frac{2n\pi y}{y_0}\right) \right]. \tag{5.5}$$

In order to satisfy the boundary conditions expressed in equation (3.9), we see that the coefficients of S_{3n}, S_{4n}, and S_{6n} must be identically zero for all n.

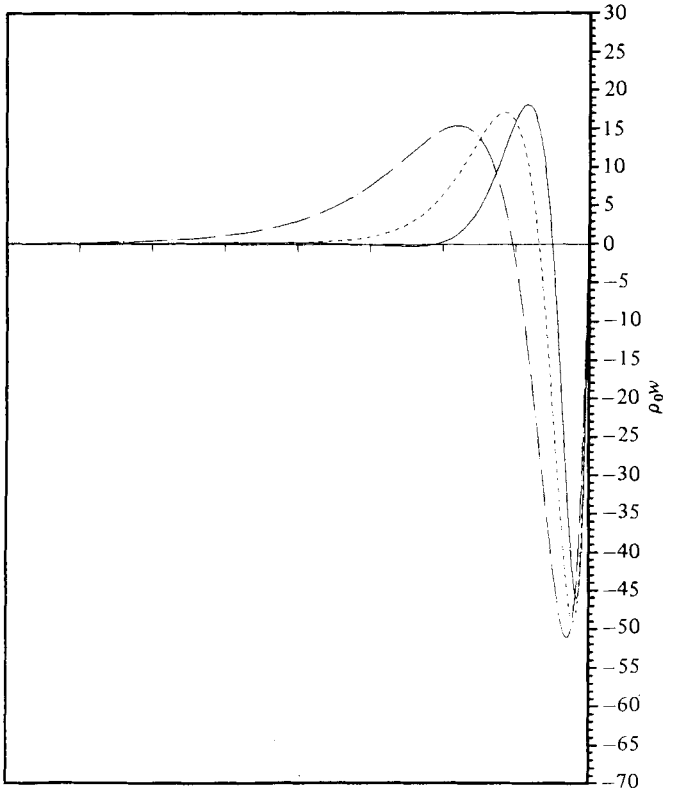

FIGURE 6. Axial mass flux (g m^{-2} s^{-1}) as a function of scale heights at the axial location $\frac{1}{4}y_0$. ——, 400 m s^{-1}; – – – –, 500 m s^{-1}; — · —, 700 m s^{-1}.

The solution of the non-homogeneous equation (2.44) can be expressed in the form

$$\chi = \chi_c + \chi_p,$$

where χ_c is the complementary solution and χ_p is the particular solution. Combining the results of equations (4.7), (5.1) and (5.5), we see that the most general form of the complementary solution is

$$\chi_c = \chi_0 + \chi_L + \chi_E. \tag{5.6}$$

The remaining coefficients of χ_0 and χ_L are determined by the boundary conditions at the rotor wall. The terms in χ_c which are constant in z are treated as the constant term of a Fourier series, and the terms in χ_c which are linear in z are used to subtract the linear dependence on z from the boundary to be decomposed by Fourier decomposition. First we treat the boundary conditions at the rotor wall ($x = 0$).

(1) $\psi(0, y) = 0$ [or, equivalently, $u(0, y) = 0$]: Since $\psi = -2A^2\chi_x$, this condition implies that

$$\sum_{j=1}^{6} a_{jn} S'_{jn}(0) = 0 \tag{5.7}$$

and

$$\sum_{j=1}^{6} b_{jn} S'_{jn}(0) = 0 \quad \text{for every } n. \tag{5.8}$$

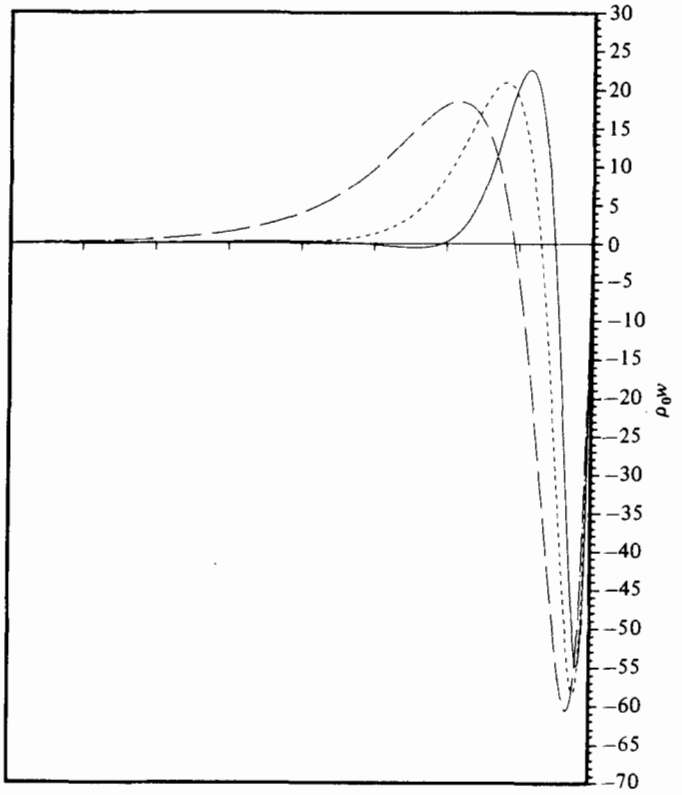

FIGURE 7. Axial mass flux (g m^{-2} s^{-1}) as a function of scale heights at the axial location $\frac{1}{2}y_0$. ——, 400 m s^{-1}; – – – –, 500 m s^{-1}; — · —, 700 m s^{-1}.

(2) $w(0,y) = 0$: Since $\rho_0 w = 4A^4\chi_{xx}$, this condition implies that

$$\sum_{j=1}^{6} a_{jn} S''_{jn}(0) = 0 \tag{5.9}$$

and

$$\sum_{j=1}^{6} b_{jn} S''_{jn}(0) = 0 \quad \textit{for every } n. \tag{5.10}$$

(3) $\phi_y(0,y) = \overline{\phi}_y(y)$: For the no internal source case, $\phi_y = (32A^{10}/Re)\, L_5\chi$, and this condition implies that

$$\frac{32A^{10}}{Re}(4c_5 y_0) = \overline{\phi}_y(y_0) - \overline{\phi}_y(0),$$

where the overbar signifies a prescribed boundary function. Solving for c_5, we find that

$$c_5 = \frac{Re}{2^7 A^{10}} \frac{\overline{\phi}_y(y_0) - \overline{\phi}_y(0)}{y_0}. \tag{5.11}$$

Similarly we have

$$\frac{32A^{10}}{Re}(4b_5) = \frac{1}{y_0}\int_0^{y_0} \left[\overline{\phi}_y(y) - \frac{2^7 A^{10}}{Re} c_5 y\right] dy = \frac{\overline{\phi}(y_0) - \overline{\phi}(0)}{y_0} - \frac{2^6 A^{10}}{Re} c_5 y_0,$$

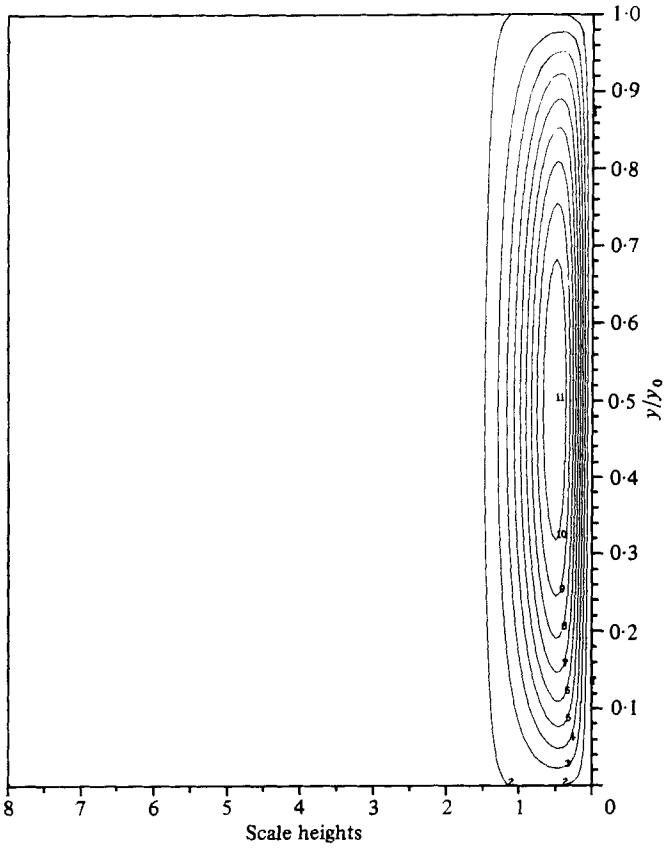

FIGURE 8. Streamlines for the 400 m s^{-1} case.

which can be solved for b_5 to give

$$b_5 = \frac{Re}{2^7 A^{10}} \frac{\overline{\phi}(y_0) - \overline{\phi}(0)}{y_0} - \tfrac{1}{2} c_5 y_0. \tag{5.12}$$

Also, we have

$$\sum_{j=1}^{6} a_{jn} L_5 S_{jn}(0) = \frac{Re}{32A^{10}} \frac{2}{y_0} \int_0^{y_0} \left[\overline{\phi}_y(y) - \frac{2^7 A^{10}}{Re} c_5 y \right] \cos \frac{2n\pi y}{y_0} \, dy \tag{5.13}$$

and

$$\sum_{j=1}^{6} b_{jn} L_5 S_{jn}(0) = \frac{Re}{32A^{10}} \frac{2}{y_0} \int_0^{y_0} \left[\overline{\phi}_y(y) - \frac{2^7 A^{10}}{Re} c_5 y \right] \sin \frac{2n\pi y}{y_0} \, dy \tag{5.14}$$

for every n. As stated earlier, $a_{jn} = b_{jn} = 0$ for $j = 3, 4, 6$ and $n = 1, 2, 3, \ldots$ in order to satisfy the interior boundary condition given by equation (3.9). However, we write the equations in a general form so that the method is clear for prescribing other boundary conditions. In any case, a sequence of linear algebraic equations must be solved to provide as many coefficients as necessary to fit the significant features of the boundary data.

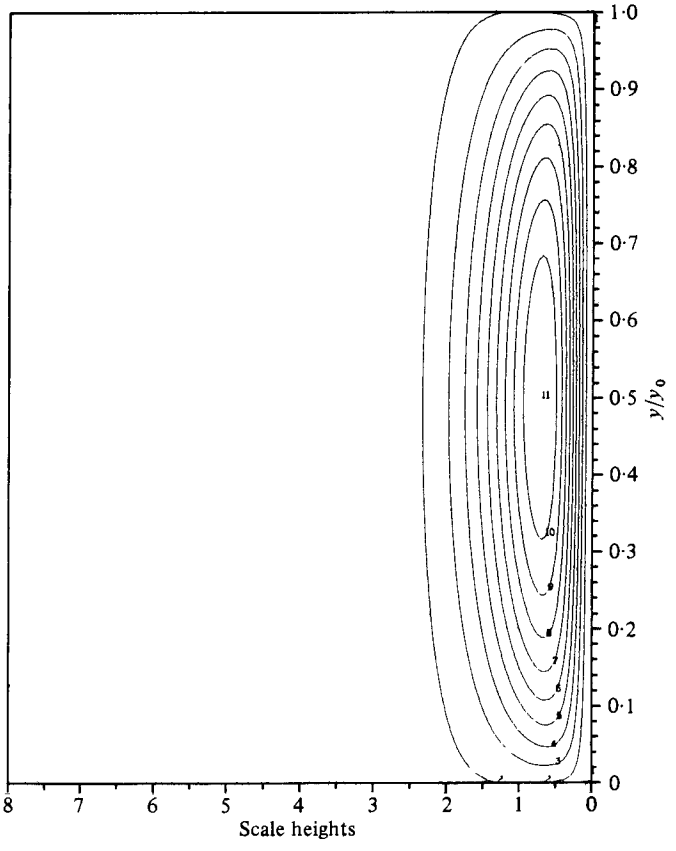

FIGURE 9. Streamlines for the 500 m s^{-1} case.

6. Ekman boundary layers

6.1. *The approximating equations*

With the centrifuge rotating about its vertical axis, boundary layers will occur on horizontal flat surfaces. These boundary layers are analogous to those first studied by Ekman (1905) in describing ocean flows. In this situation the viscous forces are balanced by the Coriolis forces and making use of this fact makes the problem quite tractable. We will follow the analysis first presented by Carrier & Maslen (1962) and later by Carrier (1964) which allows the details of the flow in the Ekman layer to be replaced by a boundary condition to be imposed on the flow outside of the Ekman layer.

While this paper was being considered by the referees, a new work by Soubbaramayer (1979) was brought to our attention. This is a very well-written article and captures some of the ideas of Onsager as described in our present work. However, Soubbaramayer, as apparently most other authors of papers on this topic, has not been aware of the work of Carrier & Maslen, which has several advantages over the approach taken by others. First, this treatment allows a much more general set of boundary conditions to be imposed on the primitive variables. For example, the Ekman solution presented by Soubbaramayer satisfies only homogeneous end conditions for the three velocity components, which precludes the cases in which a countercurrent flow is induced by a

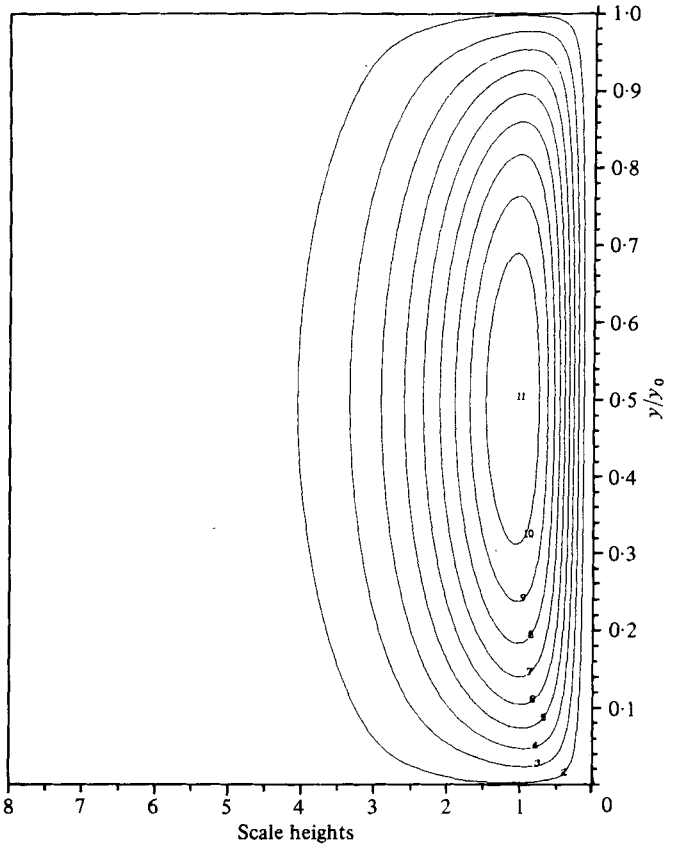

FIGURE 10. Streamlines for the 700 m s^{-1} case.

differentially rotating end wall or a mass flow through the end wall. In particular, the Carrier & Maslen treatment allows the exchange of mass between the inner and outer regions without the complication of using the so-called 'Ekman extension to the $E^{\frac{1}{3}}$ layer'. Secondly, the treatment of Carrier & Maslen avoids the complications of matching inner and outer solutions since their analysis yields a simple boundary condition to be satisfied by the flow in the region outside of the Ekman layer.

We begin the analysis with the dimensionless equations (2.10) through (2.15) and introduce a stream function Ξ by the relations

$$u = \Xi_y,$$
$$w = -\eta^{-1}(\eta\Xi)_\eta - 2A^2\eta\Xi. \tag{6.1}$$

We use equations (2.13) and (2.15) to eliminate p and ρ from equation (2.11) and we have

$$\eta\rho_0(\theta_y - 2\omega_y) = \frac{1}{Re}\left[\Delta - \frac{1}{\eta^2} - \tfrac{4}{3}A^4\eta^2\right]u_y - \frac{1}{Re}\left[\frac{\partial}{\partial\eta} - 2A^2\eta\right]\Delta w. \tag{6.2}$$

Using equation (6.1) and defining the operator $H(\Xi) = \Delta\Xi - \Xi/\eta^2$, the governing system of equations (2.12), (2.14) and (6.2) can be written as

$$2\rho_0\Xi_y = \frac{1}{Re}\left[\Delta(\eta\omega) - \omega/\eta\right], \tag{6.3}$$

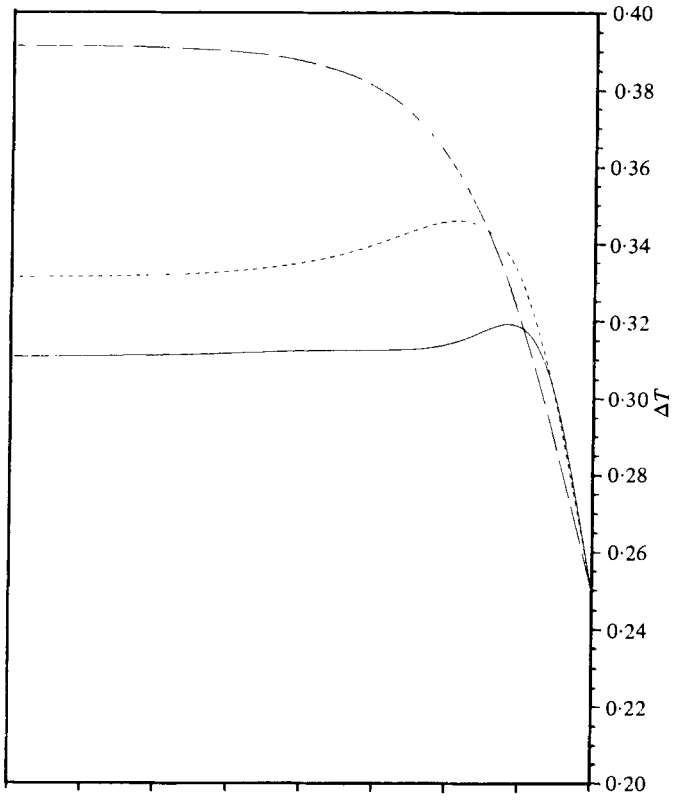

FIGURE 11. Temperature perturbation (Kelvin) as a function of scale heights at the axial location $\frac{1}{4}y_0$. ——, 400 m s^{-1}; – – – –, 500 m s^{-1}; — · —, 700 m s^{-1}.

$$4\,Re\,(S-1)\,\eta\rho_0\Xi_y = -\Delta\theta, \tag{6.4}$$

$$Re\,\eta\rho_0(\theta_y - 2\omega_y) = H^2(\Xi) + 4A^2\left[\Xi_{\eta\eta} + \frac{1}{\eta}\Xi_\eta - \frac{1}{\eta^2}\Xi\right] - 4A^4[\eta^2\Xi_{\eta\eta} + 3\eta\Xi_\eta + \Xi] - \frac{16A^4}{3}\eta^2\Xi_{yy}. \tag{6.5}$$

6.2. *Solution of the approximate equations*

We anticipate that the characterizing scale of ω, θ and Ξ in the y co-ordinate is small compared to that in the η co-ordinate. We define $\epsilon = 1/Re$ and seek solutions to the preceding equations of the form

$$\Xi(\eta, y) = \Xi_0(\eta, y) + \sqrt{(\epsilon)}\,\Xi_1\left(\eta, \frac{y}{\sqrt{\epsilon}}\right) + \sqrt{(\epsilon)}\,\Xi_2\left(\eta, \frac{y_0 - y}{\sqrt{\epsilon}}\right), \tag{6.6}$$

$$\omega(\eta, y) = \omega_0(\eta, y) + \omega_1\left(\eta, \frac{y}{\sqrt{\epsilon}}\right) + + \omega_2\left(\eta, \frac{y_0 - y}{\sqrt{\epsilon}}\right), \tag{6.7}$$

$$\theta(\eta, y) = \theta_0(\eta, y) + \theta_1\left(\eta, \frac{y}{\sqrt{\epsilon}}\right) + \theta_2\left(\eta, \frac{y_0 - y}{\sqrt{\epsilon}}\right), \tag{6.8}$$

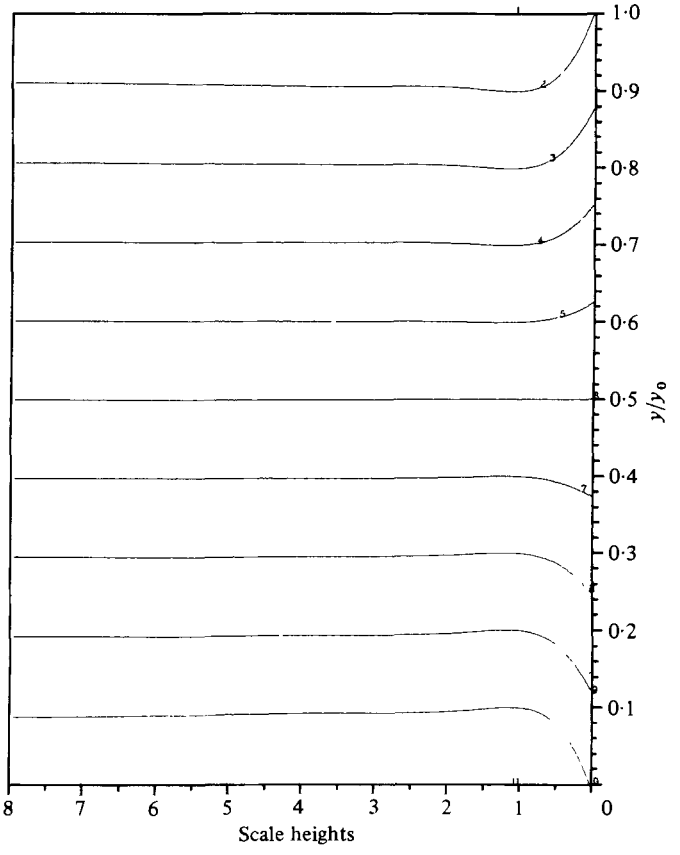

FIGURE 12. Isotherms for the 400 m s^{-1} case.

where the scales in y of the terms with subscript zero are of order unity and the scales in y of the terms with subscripts 1 and 2 are of order $\sqrt{\epsilon}$. Furthermore, the terms with subscript 1 must decay like $e^{-\xi} = e^{-y/\sqrt{\epsilon}}$ and the terms with subscript 2 must decay like $e^{-\zeta} = e^{-(y_0-y)/\sqrt{\epsilon}}$. Substituting equations (6.6) through (6.8) into equations (6.2) through (6.4), we find that the equations pertinent to the region $y = O(\sqrt{\epsilon})$ are

$$2\rho_0 \Xi_{1\xi} = \eta \omega_{1\xi\xi}, \tag{6.9}$$

$$4(S-1)\eta\rho_0 \Xi_{1\xi} = -\theta_{1\xi\xi}, \tag{6.10}$$

$$\eta\rho_0(\theta_{1\xi} - 2\omega_{1\xi}) = \Xi_{1\xi\xi\xi\xi}. \tag{6.11}$$

The first two equations can be combined to provide

$$[\theta_1 + 2(S-1)\eta^2\omega_1]_{\xi\xi} = 0 \tag{6.12}$$

and

$$[\theta_1 - 2\omega_1]_{\xi\xi} = -4[1+(S-1)\eta^2]\eta^{-1}\rho_0 \Xi_{1\xi}. \tag{6.13}$$

We define the quantities $\delta = [1+(S-1)\eta^2]^{\frac{1}{2}}$ and $\sigma = 2\rho_0\delta$ and recall that $\phi = \theta - 2\omega$.

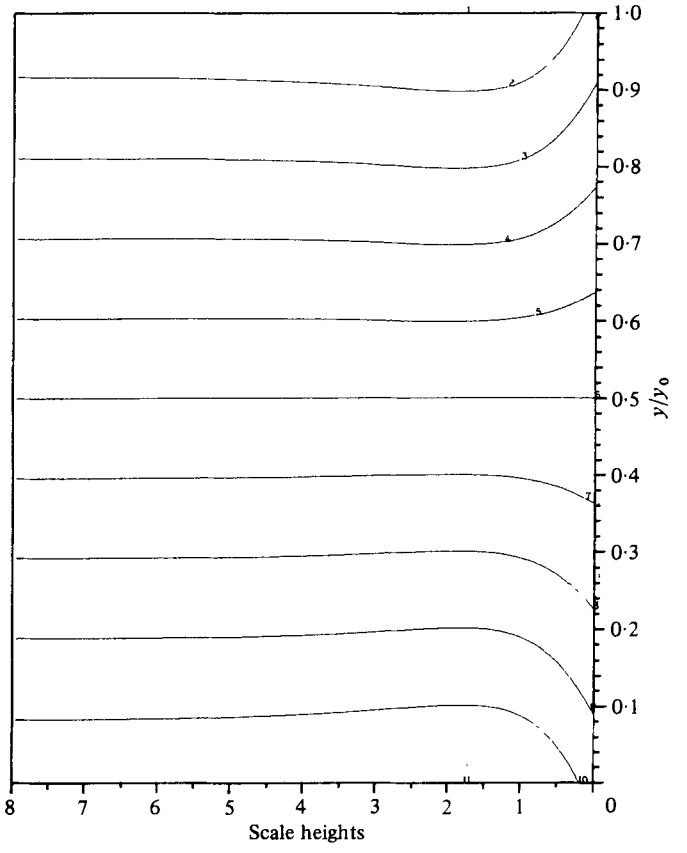

FIGURE 13. Isotherms for the 500 m s^{-1} case.

The solutions with the required exponential decay can be written

$$\Xi_1 = -\sigma^{-\frac{1}{2}}[i^{\frac{1}{2}}B_1(\eta)\,e^{-(i\sigma)^{\frac{1}{2}}\xi} + (-i)^{\frac{1}{2}}B_2(\eta)\,e^{-(-i\sigma)^{\frac{1}{2}}\xi}], \tag{6.14}$$

$$\phi_1 = -2\eta^{-1}\delta[B_1(\eta)\,e^{-(i\sigma)^{\frac{1}{2}}\xi} + B_2(\eta)\,e^{-(-i\sigma)^{\frac{1}{2}}\xi}], \tag{6.15}$$

$$\theta_1 + 2(S-1)\,\eta^2\omega_1 = C, \tag{6.16}$$

where B_1 and B_2 are functions of η to be determined from the boundary conditions and C is a constant.

6.3. *Boundary conditions*

We want to satisfy boundary conditions of the form

$$\omega = \bar{\omega}, \quad \theta = \bar{\theta}, \quad \Xi_y = \bar{U} \quad \text{and} \quad \Xi = k, \tag{6.17}$$

where $\bar{\omega}$, $\bar{\theta}$, $\bar{U}$ and k represent arbitrarily prescribed functions of η at both $y = 0$ and $y = y_0$. Using the solution as given by equations (6.14) and (6.15) and substituting into (6.6), (6.7) and (6.8) the boundary conditions yield

$$\phi(\eta, 0) = \phi_0(\eta, 0) - 2\eta^{-1}\delta[B_1(\eta) + B_2(\eta)], \tag{6.18}$$

$$i^{\frac{1}{2}}B_1(\eta) + (-i)^{\frac{1}{2}}B_2(\eta) = (\sigma\,Re)^{\frac{1}{2}}[\Xi_0(\eta, 0) - k(\eta, 0)], \tag{6.19}$$

$$iB_1(\eta) - iB_2(\eta) + \Xi_{0y}(\eta, 0) = \bar{U}(\eta, 0) \tag{6.20}$$

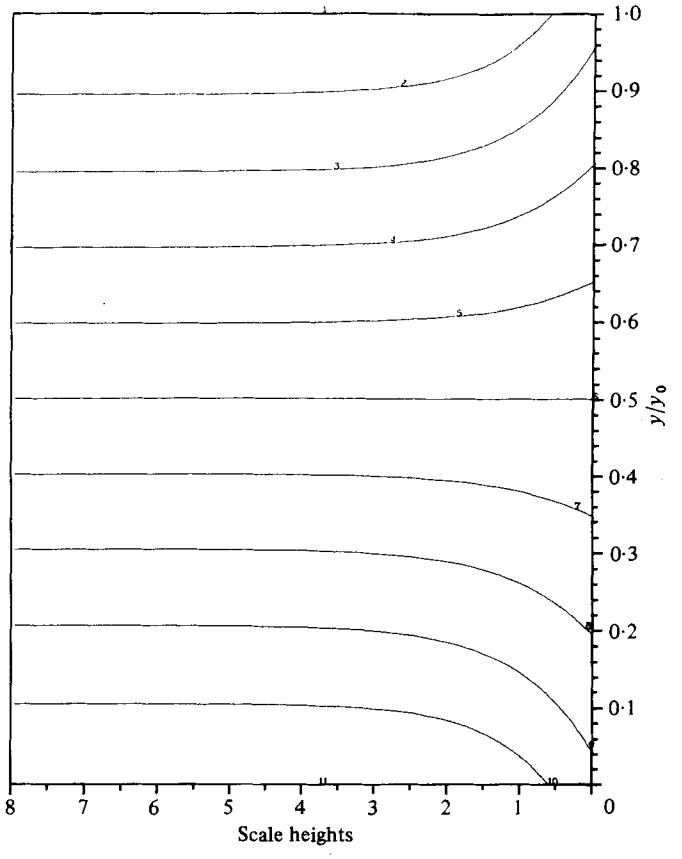

FIGURE 14. Isotherms for the 700 m s^{-1} case.

at $y = 0$. Equation (6.19) implies that $\Xi_0(0,\eta) - k(0,\eta)$ is of order $(\sigma Re)^{-\frac{1}{3}}$ times B_1 and since Ξ_{0y} cannot appreciably exceed Ξ_0 (because its y scale is of order unity) Ξ_{0y} provides a negligible contribution to equation (6.20). Therefore $B_1 = B_2 - i\overline{U}$ and, upon eliminating B_1 and B_2 between equations (6.18) and (6.19), we have a single boundary condition

$$(\rho_0 \delta Re)^{\frac{1}{3}} [\Xi_0(\eta, 0) - k(\eta, 0)] = \frac{\eta}{4\delta} [\phi_0(\eta, 0) - \overline{\phi}(\eta, 0)] + \frac{\overline{U}(\eta, 0)}{2}. \tag{6.21}$$

An identical analysis can be carried out in the vicinity of $y - y_0$ to produce the equation

$$-(\rho_0 \delta Re)^{\frac{1}{3}} [\Xi_0(\eta, y_0) - k(\eta, y_0)] = \frac{\eta}{4\delta} [\phi_0(\eta, y_0) - \overline{\phi}(\eta, y_0)] + \frac{\overline{U}(\eta, y_0)}{2}. \tag{6.22}$$

As Carrier & Maslen demonstrated, we have boundary conditions which can be applied to the interior flow field without a detailed discussion of the accompanying Ekman layers.

6.4. *Connexion with the Onsager equation*

We will make consistent approximations for equations (6.21) and (6.22) to be appropriate to the case that the interior flow is described by Onsager's model. We make the

change of variables from η to x per equation (2.16) and set $\eta = 1$ wherever it appears algebraically. This implies $\delta = S^{\frac{1}{2}}$ and $\rho_0 = e^{-x}$. Also, we replace Ξ_0, the stream function of the interior flow field, by $-\psi/\rho_0$, where ψ is the stream function appropriate to the Onsager equations and defined by equations (2.25) and (2.26). For the case that mass is removed through the boundary, we recall that $\psi(0, y) = 0$ and define

$$\dot{m}_0(x) \equiv \frac{\pi}{A^2}\int_0^x \rho_0 w(x', 0)\, dx' = -2\pi\psi(x, 0)$$

and

$$\dot{m}_{y_0}(x) \equiv \frac{\pi}{A^2}\int_0^x \rho_0 w(x', y_0)\, dx' = -2\pi\psi(x, y_0).$$

With these observations, equations (6.21) and (6.22) are replaced by

$$-4S^{\frac{3}{4}} Re^{\frac{1}{2}}\left[\psi(x, 0) + \frac{1}{2\pi}\dot{m}_0(x)\right] = e^{-\frac{1}{2}x}[\phi(x, 0) - \overline{\phi}(x, 0)] + 2S^{\frac{1}{2}} e^{-\frac{1}{2}x}\overline{U}(x, 0) \quad (6.23)$$

and

$$4S^{\frac{3}{4}} Re^{\frac{1}{2}}\left[\psi(x, y_0) + \frac{1}{2\pi}\dot{m}_{y_0}(x)\right] = e^{-\frac{1}{2}x}[\phi(x, y_0) - \overline{\phi}(x, y_0)] + 2S^{\frac{1}{2}} e^{-\frac{1}{2}x}\overline{U}(x, y_0). \quad (6.24)$$

We now substitute for ψ and ϕ in terms of the master potential in equation (5.6) and after considerable algebra express equations (6.23) and (6.24) as

$$\sum_{n=1}^{\infty} D_n p_n(x) - \sum_{n=1}^{\infty} E_n q_n(x) = R_0(x), \quad (6.25)$$

$$\sum_{n=1}^{\infty} D_n q_n(x) - \sum_{n=1}^{\infty} E_n p_n(x) = R_{y_0}(x), \quad (6.26)$$

where

$$p_n(x) = 8S^{\frac{3}{4}} Re^{\frac{1}{2}} A^2(e^{\frac{1}{2}x} f_n'(x))' - \frac{2\, Re\, S\alpha_n}{A^2} f_n(x),$$

$$q_n(x) = -\left[8S^{\frac{3}{4}} Re^{\frac{1}{2}} A^2(e^{\frac{1}{2}x} f_n'(x))' + \frac{2\, Re\, S\alpha_n}{A^2} f_n(x)\right] e^{-\alpha_n y_0}$$

and α_n and $f_n(x)$ are the eigenvalue–eigenfunction pairs discussed in § 4. The functions R_0 and R_{y_0} are determined from χ_0, χ_L and the boundary conditions and we have

$$R_0(x) = 4S^{\frac{3}{4}} Re^{\frac{1}{2}}\left\{\frac{e^{-\frac{1}{2}x}}{2A^2}[\overline{w}(x, 0) - 4A^4 e^x \chi^*_{xx}(x, 0)] + \frac{e^{\frac{1}{2}x}}{2}\left[-2A^2\chi^*_x(x, 0) + \frac{1}{2\pi}\dot{m}_0(x)\right]\right\}$$

$$-\frac{2\, Re\, S}{A^2}[\chi^*_y(x, 0) - \chi^*_y(x_T, 0)] - \overline{\phi}_x(x, 0) + 2S^{\frac{1}{2}}\overline{U}_x(x, 0),$$

$$R_{y_0}(x) = -4S^{\frac{3}{4}} Re^{\frac{1}{2}}\left\{\frac{e^{-\frac{1}{2}x}}{2A^2}[\overline{w}(x, y_0) - 4A^4 e^x \chi^*_{xx}(x, y_0)]\right.$$

$$\left. + \frac{e^{\frac{1}{2}x}}{2}\left[-2A^2\chi^*_x(x, y_0) + \frac{1}{2\pi}\dot{m}_{y_0}(x)\right]\right\} - \frac{2\, Re\, S}{A^2}[\chi^*_y(x, y_0) - \chi^*_y(x_T, y_0)]$$

$$-\overline{\phi}_x(x, y_0) + 2S^{\frac{1}{2}}\overline{U}_x(x, y_0),$$

where $\chi^* = \chi_0 + \chi_L$ and the functions $\overline{w}$, $\overline{U}$ and $\overline{\phi}$ are prescribed.

If the infinite series are truncated after N terms, equations (6.25) and (6.26) may be evaluated at a number of values of x and the coefficients D_n and E_n, $n = 1, 2, \ldots, N$, can then be determined by linear least squares. When we recall that $\chi = \chi_0 + \chi_L + \chi_E$, we see that this procedure provides a χ that meets all of the required boundary conditions even though the individual terms χ_0, χ_L, and χ_E do not necessarily. However, this procedure does have significant practical advantages. The end eigenfunctions satisfy a homogeneous problem and are free of the physical parameters, which means they can be computed and saved once and for all. The lateral eigenfunctions can be computed for classes of problems which have the same value of $\beta_n B$ and then applied to problems with a variety of boundary conditions. For example, in order to compare two centrifuges with the same value of $\beta_n B$ but different rotor-wall and/or end-wall temperature profiles, the lateral eigenfunctions would need to be computed only once.

7. Results

7.1. *Description of the calculations*

The case considered is for a centrifuge containing UF_6 with a linear wall temperature and with the temperature on the end caps constant and equal to the corresponding temperature at the cylinder wall. The geometry and operating conditions are a diameter of 18·29 cm, a length of 335·3 cm, average temperature $T_0 = 300$ K, and wall speeds of 400, 500, and 700 m/s as considered by May (1977). We will use a wall pressure of 13·3 kPa as considered by Durivault & Louvet (1976). The difference in temperature from end to end is 1 K, and for orientation the hotter end is at $y = 0$. If one wishes to consider different temperature gradients, simply multiply the results by the appropriate constant since the partial differential equation is linear.

The three cases we present are for peripheral speeds of 400, 500 and 700 metres per second. For this choice of speeds one should keep the following point in mind regarding the independent variable whose units are scale heights. The distance corresponding to one scale height in the 700 metre per second case is approximately $\frac{1}{2}$ of a scale height in the 500 m s^{-1} case and approximately $\frac{1}{3}$ of a scale height in the 400 m s^{-1} case.

All of the figures display results plotted against radial position as given in scale heights. Table 5 compares the normalized radius, η, at $x = 8$ scale heights with x at $\eta = 0{\cdot}877$ for the three speeds.

Based on the unperturbed density field, we can compute the fraction of mass contained in the first n scale heights from the cylinder wall and the mean free path at n scale heights. This information is displayed in table 6. Likewise we can compute the length of the scale heights as a function of distance from the cylinder wall. This information is displayed in table 7. From the tables we see that, in the 700 m s^{-1} case, the mean free path at 8 scale heights is about $\frac{1}{3}$ the local scale height. These tables are intended to convey a sense of appreciation of the nature of the atmosphere contained in the centrifuge and to aid in interpreting the figures.

7.2. *Discussion of results*

Figures 6 and 7 show the axial mass flux as a function of scale heights at the axial locations $\frac{1}{4}y_0$ and $\frac{1}{2}y_0$, respectively. Since $\rho_0 w$ is symmetric in the axial co-ordinate,

A^2	$\eta(x = 8)$	$x(\eta = 0{\cdot}877)$
11·29	0·540	2·6
17·64	0·739	4·1
34·57	0·877	8·0

TABLE 5. Comparison of scale heights with radial position for different speeds.

Number of scale heights	Mass fraction	Mean free path (cm)
1	0·6321	$3{\cdot}86 \times 10^{-5}$
2	0·8647	$1{\cdot}05 \times 10^{-4}$
3	0·9502	$2{\cdot}85 \times 10^{-4}$
4	0·9817	$7{\cdot}76 \times 10^{-4}$
5	0·9933	$2{\cdot}11 \times 10^{-3}$
6	0·9975	$5{\cdot}73 \times 10^{-3}$
7	0·9991	$1{\cdot}56 \times 10^{-2}$
8	0·9997	$4{\cdot}24 \times 10^{-2}$

TABLE 6. Mass fraction and mean-free-path relationship to scale height for $p_w = 13{\cdot}3$ kPa.

Scale height number	Length (cm)		
	$A^2 = 11{\cdot}29$	$A^2 = 17{\cdot}64$	$A^2 = 34{\cdot}57$
1	0·4144	0·2630	0·1332
2	0·4351	0·2710	0·1352
3	0·4592	0·2798	0·1373
4	0·4878	0·2896	0·1395
5	0·5226	0·3004	0·1418
6	0·5661	0·3125	0·1442
7	0·6226	0·3263	0·1468
8	0·7005	0·3420	0·1495

TABLE 7. Length of the scale heights related to rotation rate.

the flux at $\frac{3}{4}y_0$ will be the same as at $\frac{1}{4}y_0$. We note that the cross-over point moves away from the cylinder wall as the speed of rotation is increased.

Figures 8, 9, and 10 are the streamlines for the three cases and approximately ten per cent of the mass is contained between consecutive contours. One might recall the point made earlier that, since the length of a scale height decreases with increased rotation rate, the physical volume containing the gas is more nearly the same for the three cases than appears from the plots.

Figure 11 shows the radial dependence of the temperature perturbation as a function of scale heights at the axial location $\frac{1}{4}y_0$. The temperature is antisymmetric about the midplane so that the result at $\frac{3}{4}y_0$ is the negative of that at $\frac{1}{4}y_0$. The plots show that the perturbation increases with speed. Figures 12, 13, and 14 are the isotherms for the three cases.

The authors would like to express their appreciation to Professor George Carrier and Dr Stephen Maslen for their thoughtful comments on this manuscript. The authors would also like to express their appreciation to C. K. Carrington of the University of

Virginia and G. Sanders of Union Carbide Corporation Nuclear Division for their assistance with the calculations and the computer-generated plots.

Oak Ridge Gaseous Diffusion Plant, operated for the U.S. Department of Energy by Union Carbide Corporation, Nuclear Division under Contract W-7405 eng 26.

Appendix. Relation of the dependent variable to the master potential

$$\psi = -2A^2\chi_x, \tag{A 1}$$

$$\rho_0 u = -\psi_y - \frac{1}{2A^2}\int_0^x \mathscr{M}\,dx' = 2A^2\chi_{xy} - \frac{1}{2A^2}\int_0^x \mathscr{M}\,dx', \tag{A 2}$$

$$\rho_0 w = -2A^2\psi_x = 4A^4\chi_{xx}, \tag{A 3}$$

$$\phi_y = \frac{32A^{10}}{Re} L_5\chi + e^x\mathscr{U}_y + (e^x\mathscr{W})_x, \tag{A 4}$$

$$\phi_x = \frac{-2\,Re\,S}{A^2}[\chi_y(x,y) - \chi_y(x_T,y)] + \frac{ReS}{2A^6}\int_{x_T}^x\int_0^{x'} \mathscr{M}\,dx''\,dx' - \int_{x_T}^x (\mathscr{T} - 2\mathscr{V})\,dx. \tag{A 5}$$

REFERENCES

Avery, D. G. & Davies, E. 1973 *Uranium Enrichment by Gas Centrifuge.* London: Mills and Boon.

Bark, F. H. & Bark, T. H. 1976 On vertical boundary layers in a rapidly rotating gas. *J. Fluid Mech.* **78**, 749-761.

Brouwers, J. J. H. 1976 On the motion of a compressible fluid in a rotating cylinder. Ph.D. thesis, Twente University of Technology, Enschede, The Netherlands.

Carrier, G. F. 1964 Phenomena in rotating fluids. *Proc. 11th Int. Cong. Appl. Mech., Munich, Germany.*

Carrier, G. F. & Maslen, S. H. 1962 Flow phenomena in rapidly rotating systems. *USAEC Rep.* TID-18065.

Courant, G. & Hilbert, D. 1953 *Methods of Mathematical Physics*, vol. I. Wiley-Interscience.

Durivault, J. & Louvet, P. 1976 Etude théorique de l'écoulement dans une centrifugeuse à contre-courant thermique. *Centre d'Etudes Nucl. de Saclay, Rapport* CEA-R-4714.

Ekman, V. W. 1905 On the influence of the earth's rotation on ocean currents. *Arkiv. Mat. Astron. och Fysik* **2**, no. 11.

Erdélyi, A. 1953 *Higher Transcendental Functions*, vol. I. McGraw-Hill.

Hoglund, R. L., Shacter, J. & Von Halle, E. 1979 Diffusion separation methods. In *Encyclopedia of Chemical Technology*, vol. 7, 3rd edn (ed. R. E. Kirk & D. F. Othmer). Wiley.

LOTZ, M. 1973 Die rein axiale Strömung in einer Gegenstrom-Gasultrazentrifuge. *Atomkernenergie* **22**, 41–45.

MATSUDA, T. & HASHIMOTO, K. 1976 Thermally, mechanically or externally driven flows in a gas centrifuge with insulated horizontal end plates. *J. Fluid Mech.* **78**, 337–354.

MAY, W. G. 1977 *Separation parameters of gas centrifuges.* A.I.Ch.E. Symp. Series, no. 169, vol. 73.

OLANDER, D. R. 1972 Technical basis of the gas centrifuge. *Advances in Nuclear Science and Technology*, vol. 6. Academic.

SOUBBARAMAYER 1979 Centrifugation. In *Uranium Enrichment.* Topics in Applied Physics, vol. 35 (ed. S. Villani). Springer.

STEWARTSON, K. 1957 On almost rigid rotations. *J. Fluid Mech.* **3**, 17–26.

VILLANI, S. 1976 *Isotope Separation.* American Nuclear Society.

VON HALLE, E. 1977 The countercurrent gas centrifuge for the enrichment of U-235. *Proc. 70th Ann. Meeting A.I.Ch.E., New York* (to appear). (Also *Union Carbide Corporation, Nuclear Division, Oak Ridge, Tennessee, Rep.* K/OA-4058.)